

Article

Contribution of Regional PM_{2.5} Transport to Air Pollution Enhanced by Sub-Basin Topography: A Modeling Case over Central China

Weiyang Hu ¹, Tianliang Zhao ^{1,*}, Yongqing Bai ^{2,*}, Lijuan Shen ¹, Xiaoyun Sun ¹ and Yao Gu ¹

¹ Climate and Weather Disasters Collaborative Innovation Center, Key Laboratory for Aerosol-Cloud-Precipitation of China Meteorological Administration, PREMIC, Nanjing University of Information Science&Technology, Nanjing 210044, China; wyhu_aca@126.com (W.H.); 20181103046@nuist.edu.cn (L.S.); sunxy6362@126.com (X.S.); guyao@nuist.edu.cn (Y.G.)

² Institute of Heavy Rain, China Meteorological Administration, Wuhan 430205, China

* Correspondence: tlzhao@nuist.edu.cn (T.Z.); baiyq2007@126.com (Y.B.)

Received: 29 October 2020; Accepted: 20 November 2020; Published: 22 November 2020



Abstract: The Twain-Hu basin (THB), covering the lower plain of Hubei and Hunan provinces in Central China, has experienced severe air pollution in recent years. However, the terrain effects of such sub-basin on air quality over the THB have been incomprehensibly understood. A heavy PM_{2.5} pollution event occurred over the THB during 4–10 January 2019. By using the observations and WRF-Chem simulations, we investigated the underlying mechanisms of sub-basin effects on the air pollution with several sensitivity experiments. Observationally, air pollution in the western THB urban area with an average PM_{2.5} concentration of 189.8 $\mu\text{g m}^{-3}$, which was more serious than the eastern urban area with the average PM_{2.5} concentration of 106.3 $\mu\text{g m}^{-3}$, reflecting a different influence of topography on air pollution over the THB. Simulation results revealed that the terrain effect can contribute 12.0% to increasing the PM_{2.5} concentrations in the western THB, but slightly mitigate the pollution extent in the eastern THB with the contribution of −4.6% to PM_{2.5} during the heavy pollution episode. In particular, the sub-basin terrain was conducive to the accumulation of PM_{2.5} by regional transport with the contribution of 39.1 %, and contrarily lowered its local pollution by −57.0% via the enhanced atmospheric boundary layer height and ventilation coefficients. Given a heavy air pollution episode occurring over the THB, such inverse contribution of terrain effects reflected a unique importance of sub-basin topography in regional transport of air pollutants for air pollution in central China.

Keywords: sub-basin effect; PM_{2.5} pollution; Twain-Hu basin; regional transport; WRF-Chem

1. Introduction

For the high PM_{2.5} concentrations (i.e., the atmospheric particles with aerodynamic diameters equal to or less than 2.5 μm) in ambient atmosphere [1,2] and its negative effects on human health [3,4], PM_{2.5} variations [5,6], causes [7,8], and the impacts on environment and climate [9,10] have been intensively studied in recent years.

Anthropogenic emissions of air pollutants are the primary driver for the increase in PM_{2.5} concentrations [11,12], and unfavorable meteorological conditions are the major driver to exacerbate air pollution [13–15]. Four regions are closely associated with heavy air pollution on account of their high emission intensity—the North China Plain (NCP) [16,17], the Yangtze River Delta (YRD) [18,19] in East China, the Pearl River Delta (PRD) [20,21] in South China, and Sichuan Basin (SCB) [22–24] in Southwest China. Adverse meteorological conditions, including weak surface winds, temperature inversion layer,

and low boundary layer height, are conducive to the formation of air pollution [25]. The Chinese government has implemented a series of tailored strategies to restrict pollutant emissions [26,27], Clean Air Action for instance, to improve the atmospheric environment, or utilized wind corridors to better disperse air pollutants [28,29]. Nonetheless, compared to the anthropogenic emissions and meteorological conditions, less attention was paid to the effects of topography on air pollution.

In fact, terrain could change the meteorological conditions further influencing the air quality. Atmospheric circulation changes induced by climate warming of Tibetan Plateau (TP) result in the high frequency of air pollution in central-eastern China [30]. Moreover, it also accentuates $PM_{2.5}$ accumulations to the SCB with the impact of TP on mid-latitude westerly winds [31]. The thermal effect of the Loess Plateau can modulate the boundary layer structure to suppress the mixed layer growth and then increase air pollutants [32]. Meanwhile, the topographic effects of SCB—a unique deep basin over China intensifies the haze pollution owing to the reducing wind speed and boundary layer height, as well as the raising air temperature and humidity [31]. The lack of ventilation in the Valley of Mexico leads to high levels of air pollutants [33]. However, previous studies have not comprehensively explored the ‘sub-basin’ effects on air pollution, which should also be taken into account for polices of mitigating air pollution.

The Twain-Hu basin (THB), characterized by a sub-basin terrain, with altitudes of ~200 m in a.s.l. over central China (Figure 1a), has become a new center of air pollution [34] due to its rapid urbanization and dense population. Given the important role of topography in air quality, the reasons of $PM_{2.5}$ pollution over the sub-basin terrain of THB, should be worth investigating. Moreover, due to THB’s unique geographical location (Figure 1), air pollutants of the NCP can be transported easily to the THB driven by prevailing northerly winds of East Asian monsoons in the wintertime [35]. Meanwhile, polluted parcels would be trapped over THB given several mountains locating at the south of THB. Thus, the extent of the terrain impacts on the air pollutants, with regard to the regional transport and local pollution, needs a quantitative assessment. Moreover, how the sub-basin terrain affecting the thermal and dynamic conditions of meteorology and its relationship to air pollution also need to be further investigated.

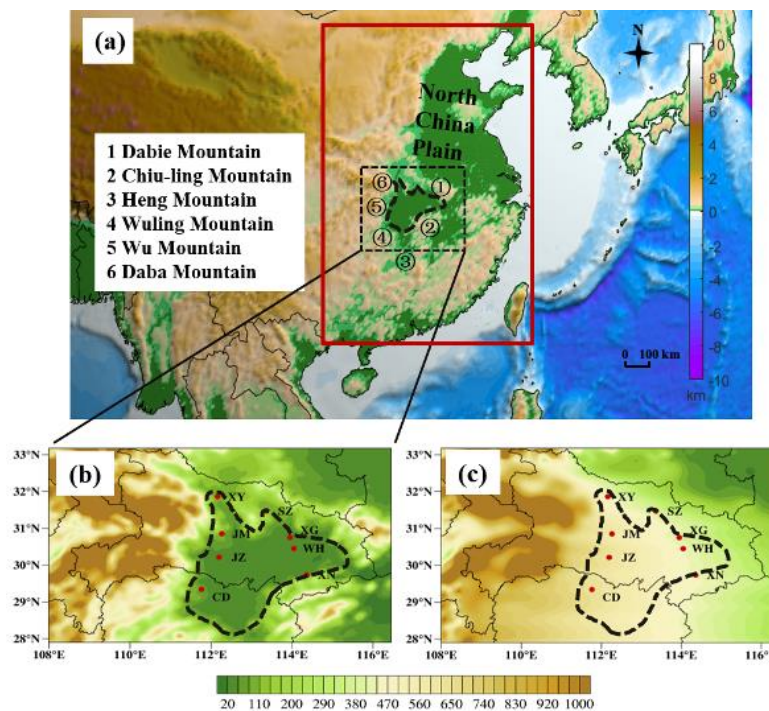


Figure 1. (a) The geographical location of the THB surround by six mountains over China [36] with the red frame covering the WRF-Chem simulation domain; (b) the terrain heights and the locations of Xiangyang (XY), Jingmen (JM), Jingzhou (JZ), Changde (CD), Suizhou (SZ), Xiaogan (XG), Wuhan (WH), and Xianning (XN) with the black dash line indicating the lower lands (mainly less than 200 m a.s.l.) around the THB; (c) the filled THB using the method of Zhang et al., 2018 [31].

This paper is organized as follows: Section 2 introduces observation data, method, and numerical experiments conducted in this paper; Section 3 describes the overall heavy air pollution event happened in the THB; Section 4 presents the results of the terrain effects on changes of the air pollutants and meteorology. Section 5 manifests the brief conclusions.

2. Data and Methods

2.1. Data

Hourly surface PM_{2.5} dataset over the THB, mainly including eight cities of Xiangyang (XY), Jingmen (JM), Jingzhou (JZ), Changde (CD), Suizhou (SZ), Xiaogan (XG), Wuhan (WH), and Xianning (XN), with terrain altitudes less than 200 m, was collected from the Chinese Ministry of Environmental Protection to discuss the heavy air pollution.

The 1° × 1° global final (FNL) reanalysis dataset from the National Center for Environment Prediction (NCEP), with a time resolution of 6 h, was used to be the initial and boundary fields of meteorological conditions for the numerical modeling. Based on observations, the vertical profile specified in chemistry routines was utilized to be the initial and lateral boundary conditions for chemistry.

Local time in China (UTC + 8:00 h) was used in this study.

2.2. Method of Filling the Terrain

In this study, we used the method of Zhang et al. 2018 [31] to fill the THB with equation:

$$H_X = H_W - (H_W - H_E) \cdot \frac{Lon_X - Lon_W}{Lon_E - Lon_W} \quad (1)$$

where H_X is the terrain height, and Lon is the longitude. Subscripts X, W, and E represent the location of filled point, west boundary of the basin, and east boundary of the high mountains, respectively. The basin-filled terrain was displayed in Figure 1c.

2.3. Model Configuration and Validation

In this study, the online-coupled WRF-Chem simulation [37] was conducted to investigate the terrain effects of the THB on the air pollution event. The simulated time was from 4 January to 10 January 2019, with hourly model outputs, and the first 24 h are considered as the spin-up. The physics parameterization schemes used comprised the Lin microphysics scheme [38], the RRTM long-wave radiation scheme [39], the Goddard shortwave scheme [40], the Mesoscale Model (MM5) similarity surface layer, the YSU boundary layer scheme [41], and the unified Noah land surface scheme [42]. In addition, the CBMZ mechanism [43,44] was employed to simulate air pollutant concentrations by using Multi-resolution Emission Inventory of China of 2016 (MEIC; <http://www.meicmodel.org/>; last accessed on 20 Nov. 2020). Detailed information of model configuration can be found in Hu et al., 2020 [45].

Some statistical metrics involving the correlation coefficient (R), the root mean square error (RMSE), mean bias (MB) and normalized mean bias (NMB) were calculated to evaluate the simulation results. As shown in Table 1, the simulation results reasonably captured the observed changes of meteorological parameters and PM_{2.5} concentrations, which therefore could be used to further study the terrain effects of the THB on air pollution event.

Table 1. Statistical metrics between observed and simulated meteorological parameters and PM_{2.5} concentrations averaged over the THB.

Variables	R	RMSE	MB	NMB (%)
T ₂ (K)	0.79	1.09	1.43	1.16
RH (%)	0.85	7.62	−6.71	−7.51
SLP (hPa)	0.93	1.35	−1.20	−0.12
WS ₁₀ (m s ^{−1})	0.68	0.27	0.06	3.18
PM _{2.5} (μg m ^{−3})	0.80	27.21	−6.39	−6.05

2.4. Numerical Experiments

In order to investigate the terrain effects on air pollution in the THB, a series of numerical experiments including E1 (control experiment, CE), E2 (transport experiment, TE), E3 (filling-hgt experiment, FHE) via filled basin (Figure 1c), and E4 (filling-hgt & transport experiment, FHE&TE) were evaluated, respectively. The differences between E1 and E3 (i.e., CE minus FHE) represent the impacts of topography on total PM_{2.5} concentrations, the experiments of E2 with E4 can evaluate the terrain influence on regional PM_{2.5} transport from upstream regions to the THB. Moreover, the potential effects of topographic effects on local PM_{2.5} pollution over THB can be identified by the differences between (E1 minus E2) and (E3 minus E4). More detailed information can be found in Table 2.

Table 2. Experimental designs in this study.

Experiments	Description
E1	Base case
E2	CE with closing all anthropogenic emissions over the THB
E3	CE with filling topography of the THB
E4	FHE with closing all anthropogenic emissions over the THB

3. Descriptions of a Heavy Air Pollution Episode

As shown in Figure 2, the THB region suffered a heavy air pollution from 4 January to 10 January 2019. All eight cities experienced high PM_{2.5} concentrations exceeding 150 μg m^{−3} with longer duration time for the western cities (XY, JM, JZ, and CD in Figure 1) compared with those in the eastern cities (SZ, XG, WH, and XN in Figure 1). During the episode process, the mean PM_{2.5} concentrations in the western and eastern cities were 189.8 and 106.3 μg m^{−3}, respectively, both well above the ‘polluted’ threshold of 75 μg m^{−3} following the ambient air quality standards of China (GB3095-2012). In addition to investigate the terrain effect on the overall PM_{2.5} concentrations, how sub-basin terrain affecting the regional transport of PM_{2.5} and its local pollution needs a quantitative evaluation, considering the special geographical location of THB.

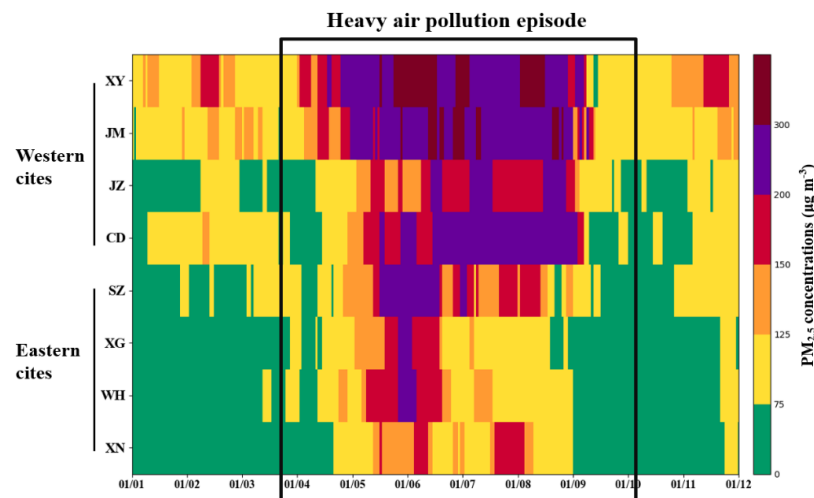


Figure 2. Hourly changes of $PM_{2.5}$ concentrations at 8 cities of XY, JM, JZ, CD, SZ, XG, WH, and XN (as shown in Figure 1), with the black frame indicating the heavy air pollution event over the THB.

4. Results and Discussion

4.1. Topographic Effects on the $PM_{2.5}$ Change in the THB

4.1.1. Potential Effects on Overall Air Quality to the THB

In order to explore the sub-basin effects on the air quality over the THB, we conducted the simulation experiments in real and changed terrain (E1 and E3 in Table 2). Figure 3 displayed the spatial distribution of $PM_{2.5}$ concentrations and wind fields averaged from 4 January to 10 January 2019 in the aforementioned simulations. Overall, the simulated $PM_{2.5}$ pollution was more serious in the western cities compared with the eastern cities (Figure 3a), consistent with the observations (Figure 2). By comparison of Figure 3a,b, the sub-basin terrain was more conducive to the accumulation of regionally transported $PM_{2.5}$ from upwind areas to the western cities in view of the big terrain gap of the northwestern THB and obvious terrain blocking of the southwestern THB (Figure 1).

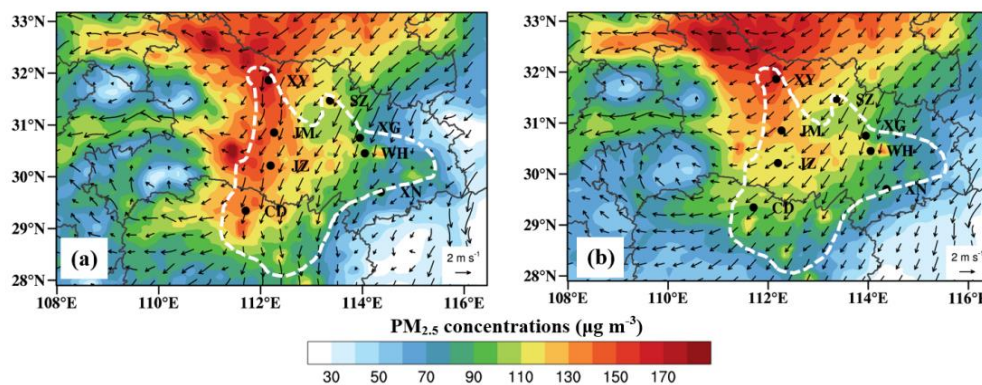


Figure 3. Distributions of the averaged near-surface $PM_{2.5}$ concentrations (color shading) and wind fields (arrows) during 4–9 January 2019 in (a) control experiment (CE) and (b) rising-hgt experiment (RHE).

Figure 4 further illustrates the differences of near-surface $PM_{2.5}$ concentrations between the E1 and E3, which further revealed that such sub-basin terrain could deteriorate the air quality with the increase in $PM_{2.5}$ by 10–40 $\mu g m^{-3}$ in the western cities. It was worth noting that the topography could slightly mitigate the air pollution in small areas of eastern cities with the $PM_{2.5}$ decrease by 0–10 $\mu g m^{-3}$, mostly because of the topographic block of the Dabie Mountain (Figure 1) weakening the invasion of air pollutants from outside, considering horizontal transport of $PM_{2.5}$ was the dominant process

in the long-range transport from the upwind sources over northern China to the receptor region of THB over central China [45]. Unexpectedly, the sub-basin terrain could also worsen the air quality of downwind areas which located in the southwest to the THB with increasing $PM_{2.5}$ concentrations by 30–50 $\mu\text{g m}^{-3}$.

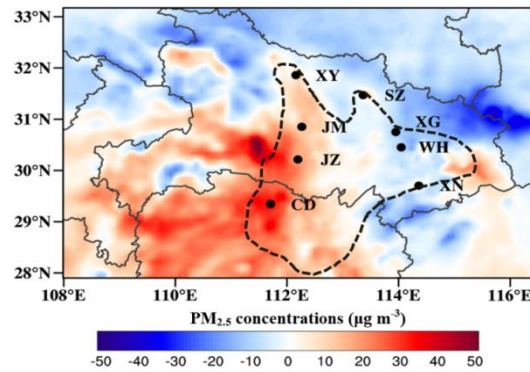


Figure 4. Distribution of near-surface $PM_{2.5}$ difference between real terrain and changed terrain simulations (CE and RHE, respectively).

On average, the sub-basin topography forced an increase in $PM_{2.5}$ concentrations by 17.4 $\mu\text{g m}^{-3}$, corresponding to 12.0% in contribution proportion in the western THB (Table S1), while the $PM_{2.5}$ level in the eastern THB was contrarily alleviated with the contribution of -4.6% . Overall, the sub-basin topography played an important role in worsening the air quality of the THB with an average contribution of 5.2% in the typical eight cities.

Vertically, the $PM_{2.5}$ concentrations averaged regionally over the THB, shown nonlinear decreases with height in both of the experiments, E1 and E3 (Figure 5). Moreover, since the effect of sub-basin topography, the $PM_{2.5}$ concentrations mostly concentrated below 2.4 km in the E1 (blue dotted line), and were more obvious below 1.9 km in the E3 (purple dotted line) without the basin effect, suggesting the great influence of the sub-basin terrain exerting on the diffusion height of the air pollutants. The vertical difference of $PM_{2.5}$ (red dotted line) among E1 and E3 further demonstrated that the deviation increased stably in the near the ground and then obviously went up between 0.6 and 0.9 km, after which it declined monotonously from 1.0 to 3.0 km with peak $PM_{2.5}$ difference of 15.2 $\mu\text{g m}^{-3}$ at 0.9 km, possibly due to the peak difference of $PM_{2.5}$ flux (Figure S1), terrain contribution accounting for 28.1%. As a whole, the THB's topography could aggravate the air quality in different heights, especially at 0.9 km, in the planetary boundary layer height (PBLH).

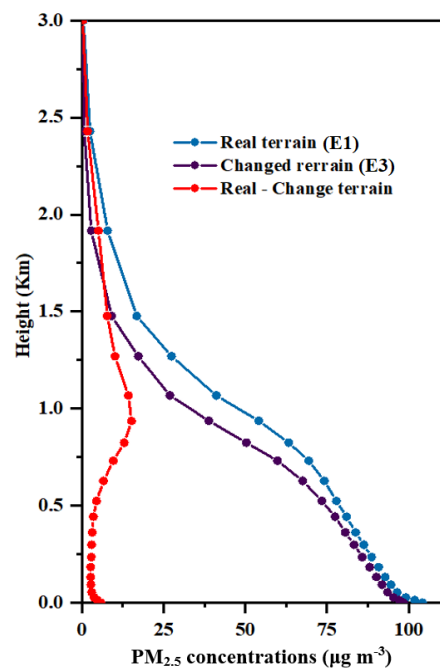


Figure 5. Vertical distribution of the averaged $PM_{2.5}$ levels in real terrain (E1; blue dotted line) and changed terrain (E3; purple dotted line) simulations and their difference (red dotted line).

4.1.2. Potential Effects on Regional Transport and Local Pollution of $PM_{2.5}$ in the THB

Figure 6 presents the distribution of near-surface $PM_{2.5}$ differences—the differences between $PM_{2.5}$ concentrations simulated by the control experiments and various sensitivity experiments (Table 2) with regard to the regional transport (RT) and local pollution (LP) respectively. It was found that the sub-basin terrain was generally in favor of the $PM_{2.5}$ accumulation of RT to THB with notable $PM_{2.5}$ increase by 5 to 60 $\mu\text{g m}^{-3}$ from east to west. The sub-basin terrain contributed about 39.1% to the RT of $PM_{2.5}$ (Table S2), with higher contribution in the western cities (48.6 %) compared with the eastern cities (29.0 %), confirming that the western cities could be more influenced by regional $PM_{2.5}$ transport from NCP triggered by East Asian winter monsoon whereas led to the mitigation of $PM_{2.5}$ pollution in the eastern cities (Figure 4) under such basin topography—the several mountains in the south and Dabie Mountain in the northeast (Figure 1a) that blocked the dispersion of air pollutants in the THB and meantime moderated the invasion of air pollutants from the outside to the eastern cities, respectively. In particular, such sub-basin topography could unexpectedly alleviate the $PM_{2.5}$ concentrations of LP by -45 – $5 \mu\text{g m}^{-3}$ during the heavy pollution process over the most areas of the THB, with contributions of 57.0% (58.1% and 55.9% in the western and eastern cities, respectively) (Table S2).

Given that the important role of the sub-basin terrain in $PM_{2.5}$ of regional transport to the THB, we further investigated the terrain contribution to the RT of $PM_{2.5}$ under different $PM_{2.5}$ pollution levels: light air pollution ($75 \mu\text{g m}^{-3} \leq PM_{2.5} < 150 \mu\text{g m}^{-3}$) and heavy air pollution ($PM_{2.5} \geq 150 \mu\text{g m}^{-3}$), according to the ambient air quality standards of China (GB3095-2012). Generally, the sub-basin topography contributed 48.3% to the RT of $PM_{2.5}$ in the light pollution level over THB, while such contribution slightly descended to 41.8% in the heavy pollution level, which implied the prevailing role of the sub-basin terrain during the air pollution process over the THB.

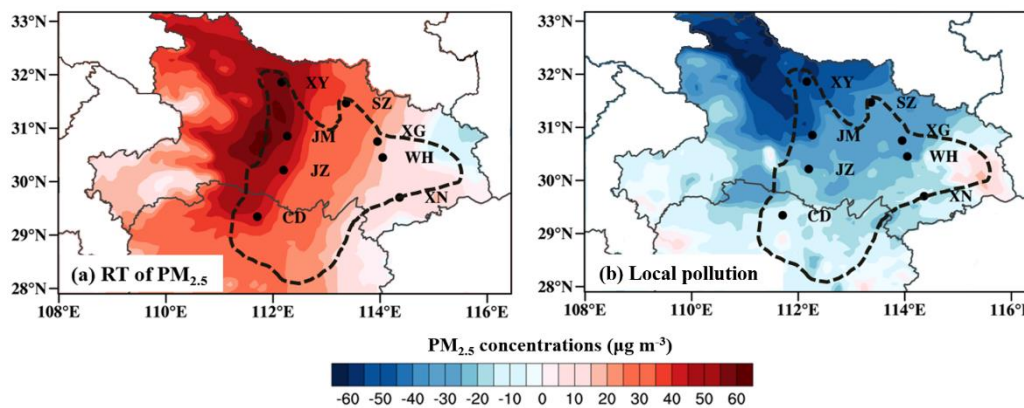


Figure 6. Distribution of near-surface $PM_{2.5}$ differences concerning (a) regional transport and (b) local pollution, respectively.

4.2. Underlying Mechanisms of Sub-Basin Terrain Influencing the Air Pollution Event

Figure 7 shows the differences of meteorology including PBLH, ventilation coefficient (VC), air temperature (T) and relative humidity (RH) between the experiments E1 and E3. In real terrain, the PBLH increased by about 30–140 m over most of the THB region (Figure 7a), resulting from the elevated height of the temperature inversion layer forced by the sub-basin terrain (Figure S2). However, the spatial distribution of such increase in PBLH exhibited great differences, with higher enhancement up to 100–140 m in the eastern cities and smaller increase by 30–60 m in the western cities where the PBLH even declined by 10–30 m, which attributed to the obvious differences of $PM_{2.5}$ pollution between the western and eastern cities (Figures 2 and 4). Positive changes of VC, ranging from 120–360 $m^{-2} s^{-2}$ over most of the THB in the real terrain (Figure 7b), could favor the regional pollutant transport from upwind areas to THB as well as the removal of local pollutants. Higher temperature and lower RH were contrarily noticed in real terrain, respectively (Figure 7c,d). Although enhanced temperature would accelerate chemical reaction of secondary aerosol, lower RH can effectively inactivate the secondary aerosol formation [46], leading to an offset of $PM_{2.5}$ concentration changes. The obvious precipitation only happened in the end of air pollution, and THB's terrain effect on precipitation could contribute 30.7% reducing rainfall over the THB, reflecting the decreased contribution of $PM_{2.5}$ precipitation washout to air pollution by sub-basin topography, which indicated that $PM_{2.5}$ concentrations can be better cleared away without sub-basin terrain.

The meteorology alteration by topography revealed the complexity of sub-basin effects on the air quality over THB and we did only investigate the terrain effect without the impact of underlying surface on the regional air pollution, which could be further studied.

Horizontal and vertical transports of $PM_{2.5}$ concentrations were two major processes in this heavy air pollution episode, and the horizontal transport of $PM_{2.5}$ was the dominant process in the long-range transport from the upwind sources over northern China to the receptor region of THB [45], while vertical transport was the process of vertical mixing of air pollutants including $PM_{2.5}$ from the upper layer downwards to the near-surface layer leading to air pollution over the receptor region of THB, which could be more important for sub-basin effects in the local scale and a direct way.

However, it was worth noting that sub-basin terrain could mitigate the local $PM_{2.5}$ pollution over THB via the increased PBLH and VC. Nevertheless, under such topography, air pollution was still exacerbated with high levels of $PM_{2.5}$ persisting over THB, suggesting the important effect of sub-basin terrain on driving $PM_{2.5}$ deterioration of regional (horizontal) transport to worsen the air quality in the THB, which was more significant in the western cities.

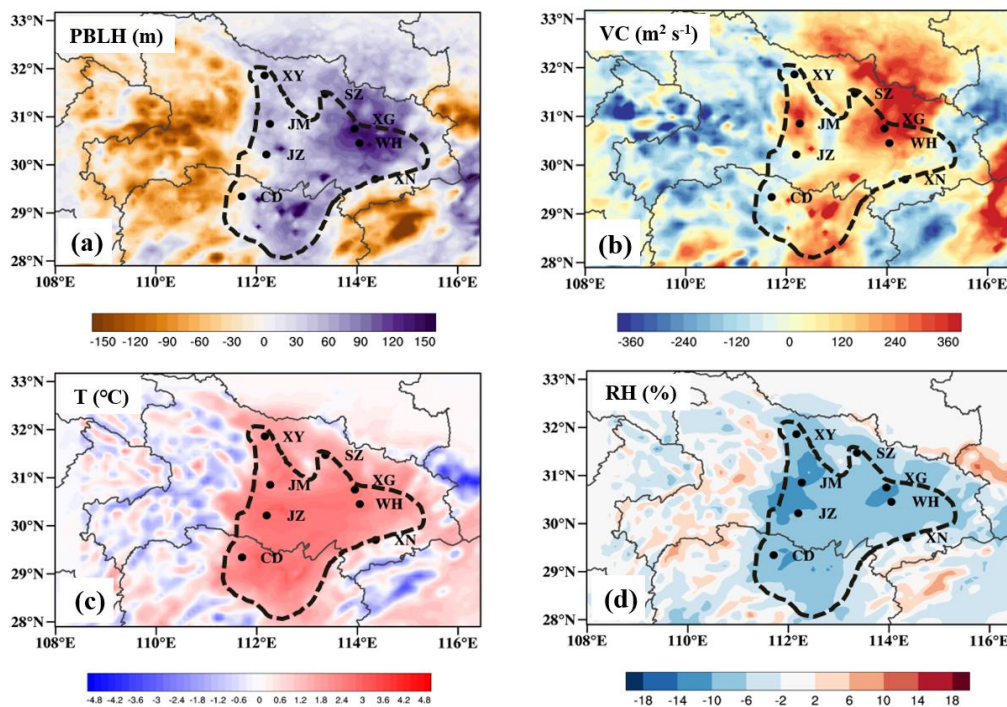


Figure 7. Near-surface differences of (a) planetary boundary layer height (PBLH; m), (b) ventilation coefficient (VC; $\text{m}^2 \text{s}^{-1}$), (c) air temperature (T ; $^{\circ}\text{C}$), and (d) relative humidity (RH; %) between real terrain (E1) and changed terrain (E3) simulations.

5. Conclusions

From 4 January to 10 January 2019, the THB experienced a heavy air pollution event, which was more serious in the western cities, with an average $\text{PM}_{2.5}$ concentration of $189.8 \mu\text{g m}^{-3}$, compared with the eastern cities (the average $\text{PM}_{2.5}$ of $106.3 \mu\text{g m}^{-3}$). In this study, four simulation experiments—including E1 (control experiment, CE), E2 (transport experiment, TE), E3 (filling-hgt experiment, FHE), and E4 (filling-hgt & transport experiment, FHE&TE)—were conducted by WRF-Chem model to evaluate the effects of the sub-basin topography on the air quality over THB, central China.

The comparison of E1 and E3 simulations revealed that the sub-basin terrain totally contributed 5.2% $\text{PM}_{2.5}$ worsening the air quality of typical 8 cities over THB. In particular, such terrain can contribute 12.0% to the $\text{PM}_{2.5}$ concentrations in the western cities, but slightly mitigated the air pollution in eastern cities with the contribution of -4.6% . Vertically, the terrain effects were more substantial at around 0.9 km with the peak $\text{PM}_{2.5}$ difference of $15.2 \mu\text{g m}^{-3}$, contributing about 28.1%.

Differences of the E2 and E4 experiments indicated that the sub-basin terrain was conducive to the $\text{PM}_{2.5}$ accumulation of RT with the average contribution of 39.1%, which was more significant in the western cities (48.6%) compared with the eastern cities (29.0%), while the THB's topography could mitigate the local $\text{PM}_{2.5}$ pollution by 57.0% over THB via the increased PBLH and VC. However, the air quality was still exacerbated with high levels of $\text{PM}_{2.5}$ persisting over THB, suggesting the outstanding important role of deteriorated $\text{PM}_{2.5}$ of regional transport by sub-basin terrain over the THB.

This study revealed that the meteorology altered by topography can alleviate the local $\text{PM}_{2.5}$ pollution over THB. However, a substantial increase in $\text{PM}_{2.5}$ concentrations exceptionally reflected the important role of sub-basin topography driving increasing $\text{PM}_{2.5}$ of regional transport to worsen the air quality over the THB.

Note that in this study near-surface $\text{PM}_{2.5}$ concentrations were resulted from the combined action of physical and chemical processes (e.g., advection, dry deposition, turbulent diffusion, cloud and

aerosol chemistry, wet scavenging, etc.) without separating every process to evaluate their difference of contribution to PM_{2.5} before and after filling the sub-basin terrain, which could be further studied.

Supplementary Materials: The following are available online at <http://www.mdpi.com/2073-4433/11/11/1258/s1>, Figure S1: Vertical distribution of difference of PM_{2.5} flux averaged over the THB during the air pollution event in real terrain and changed terrain simulations; Figure S2: Vertical distribution of temperature averaged over the THB during the air pollution event in real terrain (E1; black dotted line) and changed terrain (E3; red dotted line) simulations; Table S1: PM_{2.5} change and terrain contribution based on the E1 and E3 simulations; Table S2: Terrain contribution to regional transport of PM_{2.5} and local pollution.

Author Contributions: Conceptualization, T.Z. and Y.B.; Data curation, X.S.; Formal analysis, W.H.; Investigation, Y.G.; Resources, L.S.; Visualization, W.H.; Writing—original draft, W.H.; Writing—review and editing, T.Z. and Y.B. All authors have read and agreed to the published version of the manuscript.

Funding: This research has been supported by the National Natural Science Foundation of China (grant no. 41830965, 42075186, 91744209), and the Postgraduate Research & Practice Innovation Program of Jiangsu Province (KYCX20_0951).

Acknowledgments: This study was jointly funded by the National Natural Science Foundation of China (41830965; 42075186; 91744209), the National Key R&D Program Pilot Projects of China (2016YFC0203304), and the Postgraduate Research & Practice Innovation Program of Jiangsu Province (KYCX20_0951).

Conflicts of Interest: The authors declare no conflict of interest.

Data Availability: The data used in this paper can be provided by Weiyang Hu (wyhu_aca@126.com) upon request.

References

1. Huang, R.J.; Zhang, Y.; Bozzetti, C.; Ho, K.F.; Cao, J.J.; Han, Y.; Daellenbach, K.R.; Slowik, J.G.; Platt, S.M.; Canonaco, F.; et al. High secondary aerosol contribution to particulate pollution during haze events in china. *Nature* **2014**, *514*, 218–222. [[CrossRef](#)] [[PubMed](#)]
2. Lin, C.Q.; Liu, G.; Lau, A.K.H.; Li, Y.; Li, C.C.; Fung, J.C.H.; Lao, X.Q. High-resolution satellite remote sensing of provincial PM_{2.5} trends in China from 2001 to 2015. *Atmos. Environ.* **2018**, *180*, 110–116. [[CrossRef](#)]
3. Apte, J.S.; Marshall, J.D.; Cohen, A.J.; Brauer, M. Addressing global mortality from ambient PM_{2.5}. *Environ. Sci. Technol.* **2015**, *49*, 8057–8066. [[CrossRef](#)] [[PubMed](#)]
4. Meng, X.; Zhang, Y.; Yang, K.Q.; Yang, Y.K.; Zhou, X.L. Potential harmful effects of PM_{2.5} on occurrence and progression of acute coronary syndrome: Epidemiology, mechanisms, and prevention measures. *Int. J. Environ. Res. Public Health* **2016**, *13*, 748. [[CrossRef](#)] [[PubMed](#)]
5. Zhao, H.; Che, H.; Zhang, X.; Ma, Y.; Wang, Y.; Wang, H.; Wang, Y. Characteristics of visibility and particulate matter (PM) in an urban area of Northeast China. *Atmos. Pollut. Res.* **2013**, *4*, 427–434. [[CrossRef](#)]
6. Wang, Y.Q.; Zhang, X.Y.; Sun, J.Y.; Zhang, X.C.; Che, H.Z.; Li, Y. Spatial and temporal variations of the concentrations of PM₁₀, PM_{2.5} and PM₁ in China. *Atmos. Chem. Phys.* **2015**, *15*, 13585–13598. [[CrossRef](#)]
7. Huang, Y.; Deng, T.; Li, Z.; Wang, N.; Yin, C.; Wang, S.; Fan, S. Numerical simulations for the sources apportionment and control strategies of PM_{2.5} over Pearl River Delta, China, part I: Inventory and PM_{2.5} sources apportionment. *Sci. Total Environ.* **2018**, *634*, 1631–1644. [[CrossRef](#)]
8. Liu, B.; Song, N.; Dai, Q.; Mei, R.; Sui, B.; Bi, X.; Feng, Y. Chemical composition and source apportionment of ambient PM_{2.5} during the non-heating period in Taian, China. *Atmos. Res.* **2016**, *170*, 23–33. [[CrossRef](#)]
9. Li, Z.; Lau, W.M.; Ramanathan, V.; Wu, G.; Ding, Y.; Manoj, M.G.; Liu, J.; Qian, Y.; Li, J.; Zhou, T.; et al. Aerosol and monsoon climate interactions over Asia. *Rev. Geophys.* **2016**, *54*, 866–929. [[CrossRef](#)]
10. Rosenfeld, D.; Sherwood, S.; Wood, R.; Donner, L. Climate effects of aerosol-cloud interactions. *Science* **2014**, *343*, 379–380. [[CrossRef](#)]
11. Gui, K.; Che, H.; Wang, Y.; Wang, H.; Zhang, L.; Zhao, H.; Zheng, Y.; Sun, T.; Zhang, X. Satellite-derived PM_{2.5} concentration trends over Eastern China from 1998 to 2016: Relationships to emissions and meteorological parameters. *Environ. Pollut.* **2019**, *247*, 1125–1133. [[CrossRef](#)] [[PubMed](#)]
12. Zhang, L.; Zhao, T.; Gong, S.; Kong, S.; Tang, L.; Liu, D.; Wang, Y.; Jin, L.; Shan, Y.; Tan, C.; et al. Updated emission inventories of power plants in simulating air quality during haze periods over East China. *Atmos. Chem. Phys.* **2018**, *18*, 2065–2079. [[CrossRef](#)]

13. Zhang, X.; Zhong, J.; Wang, J.; Wang, Y.; Liu, Y. The interdecadal worsening of weather conditions affecting aerosol pollution in the Beijing area in relation to climate warming. *Atmos. Chem. Phys.* **2018**, *18*, 5991–5999. [[CrossRef](#)]
14. Xu, X.; Wang, Y.; Zhao, T.; Cheng, X.; Meng, Y.; Ding, G. “Harbor” effect of large topography on haze distribution in eastern China and its climate modulation on decadal variations in haze. *Chin. Sci. Bull.* **2015**, *60*, 1132–1143.
15. Zhong, J.; Zhang, X.; Dong, Y.; Wang, Y.; Liu, C.; Wang, J.; Zhang, Y.; Che, H. Feedback effects of boundary-layer meteorological factors on cumulative explosive growth of PM_{2.5} during winter heavy pollution episodes in Beijing from 2013 to 2016. *Atmos. Chem. Phys.* **2018**, *18*, 247. [[CrossRef](#)]
16. Cao, Z.; Sheng, L.; Liu, Q.; Yao, X.; Wang, W. Interannual increase of regional haze-fog in North China Plain in summer by intensified easterly winds and orographic forcing. *Atmos. Environ.* **2015**, *122*, 154–162.
17. Zhao, H.; Che, H.; Zhang, L.; Gui, K.; Ma, Y.; Wang, Y.; Wang, H.; Zheng, Y.; Zhang, X. How aerosol transport from the North China plain contributes to air quality in northeast China. *Sci. Total Environ.* **2020**, *738*, 139555. [[CrossRef](#)]
18. Hua, Y.; Cheng, Z.; Wang, S.; Jiang, J.; Chen, D.; Cai, S.; Fu, X.; Fu, Q.; Chen, C.; Xu, B.; et al. Characteristics and source apportionment of PM_{2.5} during a fall heavy haze episode in the Yangtze River Delta of China. *Atmos. Environ.* **2015**, *123*, 380–391. [[CrossRef](#)]
19. Wang, M.; Cao, C.; Li, G.; Singh, R.P. Analysis of a severe prolonged regional haze episode in the Yangtze River Delta, China. *Atmos. Environ.* **2015**, *102*, 112–121. [[CrossRef](#)]
20. Deng, X.; Tie, X.; Wu, D.; Zhou, X.; Bi, X.; Tan, H.; Li, F.; Jiang, C. Long-term trend of visibility and its characterizations in the Pearl River Delta (PRD) region, China. *Atmos. Environ.* **2008**, *42*, 1424–1435. [[CrossRef](#)]
21. Wang, X.; Chen, W.; Chen, D.; Wu, Z.; Fan, Q. Long-term trends of fine particulate matter and chemical composition in the Pearl River Delta Economic Zone (PRDEZ), China. *Front. Environ. Sci. Eng.* **2016**, *10*, 53–62. [[CrossRef](#)]
22. Liao, T.; Wang, S.; Ai, J.; Gui, K.; Duan, B.; Zhao, Q.; Zhang, X.; Jiang, W.; Sun, Y. Heavy pollution episodes, transport pathways and potential sources of PM_{2.5} during the winter of 2013 in Chengdu (China). *Sci. Total Environ.* **2017**, *584–585*, 1056–1065. [[CrossRef](#)] [[PubMed](#)]
23. Wang, J.; Zhao, B.; Wang, S.; Yang, F.; Xing, J.; Morawska, L.; Ding, A.; Kulmala, M.; Kerminen, V.-M.; Kujansuu, J.; et al. Particulate matter pollution over China and the effects of control policies. *Sci. Total Environ.* **2017**, *584–585*, 426447.
24. Ning, G.; Wang, S.; Ma, M.; Ni, C.; Shang, Z.; Wang, J.; Li, J. Characteristics of air pollution in different zones of Sichuan Basin, China. *Sci. Total Environ.* **2018**, *612*, 975–984. [[CrossRef](#)]
25. Chen, Z.; Chen, D.; Zhao, C.; Kwan, M.; Cai, J.; Zhuang, Y.; Zhao, B.; Wang, X.; Chen, B.; Xu, B. Influence of meteorological conditions on PM_{2.5} concentrations across China: A review of methodology and mechanism. *Environ. Int.* **2020**, *139*, 105558. [[CrossRef](#)]
26. Qiu, J. Fight against smog ramps up. *Nature* **2014**, *506*, 273–274. [[CrossRef](#)]
27. Zhang, Q.; He, K.; Huo, H. Policy: Cleaning China’s air. *Nature* **2012**, *484*, 161–162. [[CrossRef](#)]
28. Ren, C.; Yang, R.; Cheng, C.; Xing, P.; Fang, X.; Zhang, S.; Wang, H.; Shi, Y.; Zhang, X.; Kwok, Y.T.; et al. Creating breathing cities by adopting urban ventilation assessment and wind corridor plan—The implementation in Chinese cities. *J. Wind Eng. Ind. Aerod.* **2018**, *182*, 170–188. [[CrossRef](#)]
29. Yuan, C.; Ng, E.; Norford, L.K. Improving air quality in high-density cities by understanding the relationship between air pollutant dispersion and urban morphologies. *Build Environ.* **2014**, *71*, 245–258. [[CrossRef](#)]
30. Xu, X.; Zhao, T.; Liu, F.; Gong, S.L.; Kristovich, D.; Lu, C.; Guo, Y.; Cheng, X.; Wang, Y.; Ding, G. Climate modulation of the Tibetan Plateau on haze in China. *Atmos. Chem. Phys.* **2016**, *16*, 1365–1375. [[CrossRef](#)]
31. Zhang, L.; Guo, X.; Zhao, T.; Gong, S.; Xu, X.; Li, Y.; Luo, L.; Gui, K.; Wang, H.; Zheng, Y.; et al. A modeling study of the terrain effects on haze pollution in the Sichuan Basin. *Atmo. Environ.* **2019**, *196*, 77–85. [[CrossRef](#)]
32. Hu, X.-M.; Ma, Z.; Lin, W.; Zhang, H.; Hu, J.; Wang, Y.; Xu, X.; Fuentes, J.D.; Xue, M. Impact of the Loess Plateau on the atmospheric boundary layer structure and air quality in the North China Plain: A case study. *Sci. Total Environ.* **2014**, *499*, 228–237. [[CrossRef](#)] [[PubMed](#)]
33. Jazcilevich, A.D.; García, A.R.; Caetano, E. Locally induced surface air confluence by complex terrain and its effects on air pollution in the valley of Mexico. *Atmos. Environ.* **2005**, *39*, 5481–5489. [[CrossRef](#)]

34. Shen, L.; Wang, H.; Zhao, T.; Liu, J.; Bai, Y.; Kong, S.; Shu, Z. Characterizing regional aerosol pollution in central China based on 19 years of MODIS data: Spatiotemporal variation and aerosol type discrimination. *Environ. Pollut.* **2020**, *263*. [[CrossRef](#)]
35. Ding, Y. *Monsoons over China*; Springer Science & Business Media: Berlin, Germany, 1994.
36. Bezděk, A.; Sebera, J. Matlab script for 3D visualizing geodata on a rotating globe. *Comput. Geosci.* **2013**, *56*, 127–130. [[CrossRef](#)]
37. Grell, G.A.; Peckham, S.E.; Schmitz, R.; McKeen, S.A.; Frost, G.; Skamarock, W.C.; Eder, B. Fully coupled “online” chemistry within the WRF model. *Atmos. Environ.* **2005**, *39*, 6957–6975. [[CrossRef](#)]
38. Lin, Y.-L.; Farley, R.D.; Orville, H.D. Bulk Parameterization of the Snow Field in a Cloud Model. *J. Clim. Appl. Meteorol.* **1983**, *22*, 1065–1092. [[CrossRef](#)]
39. Mlawer, E.J.; Taubman, S.J.; Brown, P.D.; Iacono, M.J.; Clough, S.A. Radiative transfer for inhomogeneous atmospheres: RRTM, a validated correlated-k model for the longwave. *J. Geophys. Res. Atmos.* **1997**, *102*, 16663–16682. [[CrossRef](#)]
40. Chou, M.D.; Suarez, M.J.; Ho, C.H.; Yan, M.M.H.; Lee, K.T. Parameterizations for Cloud Overlapping and Shortwave Single-Scattering Properties for Use in General Circulation and Cloud Ensemble Models. *J. Clim.* **1998**, *11*, 202–214. [[CrossRef](#)]
41. Hong, S.-Y.; Noh, Y.; Dudhia, J. A New Vertical Diffusion Package with an Explicit Treatment of Entrainment Processes. *Mon. Weather Rev.* **2006**, *134*, 2318–2341. [[CrossRef](#)]
42. Tewari, M.; Chen, F.; Wang, W.; Dudhia, J.; Lemone, M.A.; Mitchell, K.; Ek, M.; Gayno, G.; Wegiel, J.; Cuenca, R.H. Implementation and verification of the unified NOAA land surface model in the WRF model. In Proceedings of the conference on Weather Analysis and Forecasting/conference on Numerical Weather Prediction, American Meteorological Society, Seattle, WA, USA, 14 January 2014.
43. Zaveri, R.A.; Peters, L.K. A new lumped structure photochemical mechanism for large-scale applications. *J. Geophys. Res.* **1999**, *104*, 30387. [[CrossRef](#)]
44. Zaveri, R.A.; Easter, R.C.; Fast, J.D.; Peters, L.K. Model for Simulating Aerosol Interactions and Chemistry (MOSAIC). *J. Geophys. Res.* **2008**, *113*, D13204. [[CrossRef](#)]
45. Hu, W.; Zhao, T.; Bai, Y.; Kong, S.; Xiong, J.; Sun, X.; Yang, Q.; Gu, Y.; Lu, H. Importance of Regional PM_{2.5} Transport and Precipitation Washout in Heavy Air Pollution in the Twain-Hu Basin over Central China: Observational Analysis and WRF-Chem Simulation. *Science of the Total Environment*. 2020. Available online: <https://doi.org/10.1016/j.scitotenv.2020.143710> (accessed on 20 November 2020).
46. Sun, Y.; Wang, Z.; Fu, P.; Jiang, Q.; Yang, T.; Li, J.; Ge, X. The impact of relative humidity on aerosol composition and evolution processes during wintertime in Beijing, China. *Atmos. Environ.* **2013**, *77*, 927–934. [[CrossRef](#)]

Publisher’s Note: MDPI stays neutral with regard to jurisdictional claims in published maps and institutional affiliations.



© 2020 by the authors. Licensee MDPI, Basel, Switzerland. This article is an open access article distributed under the terms and conditions of the Creative Commons Attribution (CC BY) license (<http://creativecommons.org/licenses/by/4.0/>).